Connection of temporal coupled-mode-theory formalisms for a resonant optical system and its time-reversal conjugate

Zhexin Zhao, Cheng Guo, and Shanhui Fan

Phys. Rev. A **99**, 033839 — Published 19 March 2019

DOI: 10.1103/PhysRevA.99.033839

The connection of temporal coupled mode theory formalisms for a resonant optical system and its time-reversal conjugate

Zhexin Zhao, Cheng Guo, and Shanhui Fan*
Ginzton Laboratory, 348 Via Pueblo Mall, Stanford University, CA, 94305, USA
(Dated: January 24, 2019)

Temporal coupled mode theory has been widely used to describe the physics of resonant optical systems. In general, an optical system can be constraint by energy conservation, time-reversal symmetry, and reciprocity. Most previous developments of temporal coupled mode theory made use of all three constraints. In this paper, we consider separately the implication of each of these constraints on the parameters of temporal coupled mode theory. For this purpose we made extensive use of the connection between a physical system and its time-reversal conjugate. This connection also indicates some of the non-trivial implications on the relation between the resonant properties of a physical system and its time-reversal conjugate. We validate these implications numerically by direct electromagnetic simulations of a guided resonance system. This work should enable the application of temporal coupled mode theory to a wider range of resonant systems.

I. INTRODUCTION

Resonance phenomenon is ubiquitous in optics. In an open resonant system, where the resonant mode interacts with propagation waves, the temporal coupled mode theory (TCMT) phenomenologically describes the dynamics of the resonant system [1–12]. The TCMT descriptions match with rigorous numerical simulations in resonant systems quite well [4, 5, 7, 13] and has been widely used as a guidance in the design of optical devices [14–17].

The formalism of TCMT is strongly constrained by various symmetry constraints present in the optical system. The three most commonly used ones are time-reversal symmetry [18], energy conservation and Lorentz reciprocity. For these three constraints, the presence of any two constraints imply the third [2]. Previous developments of the temporal coupled mode theory formalism typically assumed the presence of all three constraints [4, 5]. On the other hand, there are a large number of optical systems that satisfy only one of the three constraints. As one example, systems with gain and loss do not conserve energy and do not satisfy time-reversal symmetry, but are usually reciprocal [19, 20]. As another example, lossless magneto-optical systems conserve energy, but break both reciprocity and time-reversal symmetry. To provide an intuitive understanding of these systems, it would certainly be of interest to develop the temporal coupled mode theory formalism for systems where only one of the three constraints is present. Along this direction, Ref. [21] has recently discussed the implications of time-reversal symmetry and energy conservation separately. In this paper, we provide a general theoretical discussion.

For the theoretical development in this paper, we make extensive use of the connection in terms of the physical properties between a system and its time-reversal conjugate. This connection has been extensively used in the discussions of coherent perfect absorbers [22, 23], and for elucidating various consequences of parity-time symmetry [19]. Here we highlight the use of this connection in the development of TCMT.

The paper is organized as follows. In Section II, we first study the TCMT description of the time-reversal conjugate system of a general single-mode resonator system, which can have material loss or break Lorentz reciprocity. For simplicity, we limit all of our discussions to systems supporting a single resonance in the frequency range of interest. Equipped with the TCMT description of the time-reversal conjugate system, we then discuss the constrains on TCMT separately imposed by time-reversal symmetry, energy conservation and Lorentz reciprocity in Sections III-V, respectively. In Section VI, we discuss some non-intuitive relations between the original and time-reversal conjugate systems when the original system has material loss and satisfies Lorentz reciprocity, and provide numerical validations. We conclude in Section VII.

II. TCMT OF THE TIME-REVERSAL CONJUGATE SYSTEM

We consider a general electromagnetic system (referred to as the "original" system) as described by permittivity $\boldsymbol{\epsilon}(\boldsymbol{r},\omega)$ and permeability $\boldsymbol{\mu}(\boldsymbol{r},\omega)$. In the time domain, the electromagnetic fields in this system are described by the Maxwell's equations

$$\nabla \times \boldsymbol{E}(\boldsymbol{r},t) = -\frac{\partial \boldsymbol{B}(\boldsymbol{r},t)}{\partial t}, \tag{1a}$$

$$\nabla \times \boldsymbol{H}(\boldsymbol{r},t) = \frac{\partial \boldsymbol{D}(\boldsymbol{r},t)}{\partial t}, \tag{1b}$$

where $\boldsymbol{E}$, $\boldsymbol{H}$, $\boldsymbol{D}$, $\boldsymbol{B}$ are electric field, magnetic field, displacement field and magnetic induction field, respectively, and $\boldsymbol{D}(\boldsymbol{r},\omega) = \epsilon(\boldsymbol{r},\omega)\boldsymbol{E}(\boldsymbol{r},\omega)$, $\boldsymbol{B}(\boldsymbol{r},\omega) = \mu(\boldsymbol{r},\omega)\boldsymbol{H}(\boldsymbol{r},\omega)$.

* shanhui@stanford.edu

Starting from Eq. (1), we note that the fields

$$\begin{aligned}\widetilde{\boldsymbol{E}}(\boldsymbol{r},t)&=\boldsymbol{E}(\boldsymbol{r},-t),\ \widetilde{\boldsymbol{D}}(\boldsymbol{r},t)=\boldsymbol{D}(\boldsymbol{r},-t),\\ \widetilde{\boldsymbol{H}}(\boldsymbol{r},t)&=-\boldsymbol{H}(\boldsymbol{r},-t),\ \widetilde{\boldsymbol{B}}(\boldsymbol{r},t)=-\boldsymbol{B}(\boldsymbol{r},-t),\end{aligned} \tag{2}$$

also satisfy the same Maxwell's equations, i.e.

$$\nabla\times\widetilde{\boldsymbol{E}}(\boldsymbol{r},t)=-\frac{\partial\widetilde{\boldsymbol{B}}(\boldsymbol{r},t)}{\partial t}, \tag{3a}$$

$$\nabla\times\widetilde{\boldsymbol{H}}(\boldsymbol{r},t)=\frac{\partial\widetilde{\boldsymbol{D}}(\boldsymbol{r},t)}{\partial t}. \tag{3b}$$

Therefore, in principle, these fields can be realized in a physical system. We refer to such a system as the time-reversal conjugate of the original system, or "conjugate system" for brevity.

To see the permittivity and permeability distribution of such conjugate system, we notice the following relations:

$$\begin{aligned}\widetilde{\boldsymbol{D}}(\boldsymbol{r},t)=\boldsymbol{D}(\boldsymbol{r},-t)&=\int_{-\infty}^{\infty}d\omega\boldsymbol{D}(\boldsymbol{r},\omega)e^{-i\omega t}\\ &=\int_{-\infty}^{\infty}d\omega\boldsymbol{D}^*(\boldsymbol{r},\omega)e^{i\omega t}\\ &=\int_{-\infty}^{\infty}d\omega\boldsymbol{\epsilon}^*(\boldsymbol{r},\omega)\boldsymbol{E}^*(\boldsymbol{r},\omega)e^{i\omega t}\end{aligned} \tag{4}$$

$$\widetilde{\boldsymbol{E}}(\boldsymbol{r},t)=\int_{-\infty}^{\infty}d\omega\boldsymbol{E}^*(\boldsymbol{r},\omega)e^{i\omega t} \tag{5}$$

Thus,

$$\widetilde{\boldsymbol{D}}(\boldsymbol{r},\omega)=\boldsymbol{\epsilon}^*(\boldsymbol{r},\omega)\widetilde{\boldsymbol{E}}(\boldsymbol{r},\omega), \tag{6}$$

and similarly

$$\widetilde{\boldsymbol{B}}(\boldsymbol{r},\omega)=\boldsymbol{\mu}^*(\boldsymbol{r},\omega)\widetilde{\boldsymbol{H}}(\boldsymbol{r},\omega). \tag{7}$$

Therefore, the conjugate system is defined by the permittivity distribution $\boldsymbol{\epsilon}^*(\boldsymbol{r},\omega)$ and permeability distribution $\boldsymbol{\mu}^*(\boldsymbol{r},\omega)$. For simplicity, we assume $\boldsymbol{\mu}(\boldsymbol{r},\omega)=\mu_0$ in the following discussions, where μ_0 is the vacuum permeability. The generalization to systems with a permeability different from vacuum should be straightforward.

In the conjugate system, its time-dependent electromagnetic field is related to those of the original system by Eq. (2), and its frequency-domain electromagnetic field is related to those of the original system by

$$\begin{aligned}\widetilde{\boldsymbol{E}}(\boldsymbol{r},\omega)&=\boldsymbol{E}^*(\boldsymbol{r},\omega),\ \widetilde{\boldsymbol{D}}(\boldsymbol{r},\omega)=\boldsymbol{D}^*(\boldsymbol{r},\omega),\\ \widetilde{\boldsymbol{H}}(\boldsymbol{r},\omega)&=-\boldsymbol{H}^*(\boldsymbol{r},\omega),\ \widetilde{\boldsymbol{B}}(\boldsymbol{r},\omega)=-\boldsymbol{B}^*(\boldsymbol{r},\omega).\end{aligned} \tag{8}$$

We proceed to consider an original system consisting of a single-mode resonator as described by a dielectric function $\boldsymbol{\epsilon}(\boldsymbol{r})$, coupling to input and output ports, as shown in Fig. 1(a). We assume a total of m input or output ports. We assume that the input and output ports are made of energy conserving, time-reversal invariant, and reciprocal materials. We do not, however, constrain any aspect of $\boldsymbol{\epsilon}(\boldsymbol{r})$ within the resonator. This system can be described by a temporal coupled mode theory equation [4]:

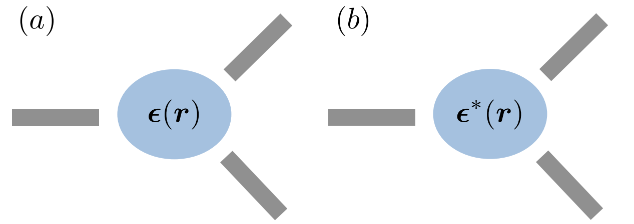

FIG. 1. (a) Schematic of a resonator system described by a dielectric function $\boldsymbol{\epsilon}(\boldsymbol{r})$, coupling to multiple ports. (b) The time-reversal conjugate system with respect to (a) is described by a dielectric function $\boldsymbol{\epsilon}^*(\boldsymbol{r})$.

$$\frac{d}{dt}a=(i\omega_0-\gamma)a+\boldsymbol{\kappa}^T\boldsymbol{s}_+, \tag{9a}$$

$$\boldsymbol{s}_-=C\boldsymbol{s}_++\boldsymbol{d}a, \tag{9b}$$

where a represents the amplitude of the resonant mode. $\boldsymbol{s}_+$ and $\boldsymbol{s}_-$ are both m dimensional column vectors, the components of which are respectively the amplitudes of the incoming and outgoing waves in the ports. $\boldsymbol{\kappa}$ ($\boldsymbol{d}$) is also an m-vector, the components of which are the coupling rates between the resonator and the incoming (outgoing) waves in the ports. C is an $m\times m$ scattering matrix that describes the background scattering process, i.e. the scattering of the system in the absence of the resonance. ω_0 and γ are the resonant frequency and decay rate of the resonant mode, respectively. Generally, the decay rate γ consists of two parts, i.e. $\gamma=\gamma_r+\gamma_i$, where $\gamma_r=\boldsymbol{d}^\dagger\boldsymbol{d}/2$ is the radiative decay rate of the resonant mode, and γ_i is the intrinsic decay rate due to the material loss.

The system conjugate to the original single-mode resonator system is described by a dielectric function $\boldsymbol{\epsilon}^*(\boldsymbol{r})$. This system can generally also be described by a temporal coupled mode theory equation:

$$\frac{d}{dt}\tilde{a}=(i\widetilde{\omega}_0-\widetilde{\gamma})\tilde{a}+\widetilde{\boldsymbol{\kappa}}^T\tilde{\boldsymbol{s}}_+, \tag{10a}$$

$$\tilde{\boldsymbol{s}}_-=\widetilde{C}\tilde{\boldsymbol{s}}_++\widetilde{\boldsymbol{d}}\tilde{a}, \tag{10b}$$

where every quantity in Eq. (10) has the same physical meaning with the corresponding quantity without the $\sim$ in Eq. (9). The mode amplitude and the amplitudes of the incoming and outgoing waves in the conjugate system are related to those in the original system through:

$$\tilde{a}(t)=a^*(-t), \tag{11}$$

$$\tilde{\boldsymbol{s}}_+(t)=\boldsymbol{s}_-^*(-t), \tag{12}$$

$$\tilde{\boldsymbol{s}}_-(t)=\boldsymbol{s}_+^*(-t). \tag{13}$$

On the other hand, directly from Eq. (9), we have

$$\frac{d}{dt}a^*(-t) = (i\omega_0 + \gamma)a^*(-t) - \boldsymbol{\kappa}^\dagger \boldsymbol{s}_+^*(-t), \tag{14a}$$

$$\boldsymbol{s}_-^*(-t) = C^*\boldsymbol{s}_+^*(-t) + \boldsymbol{d}^* a^*(-t). \tag{14b}$$

Substitute Eqs. (11 - 13) to Eq. (14), we get

$$\frac{d}{dt}\tilde{a}(t) = (i\omega_0 + \gamma + \boldsymbol{\kappa}^\dagger C^{*-1}\boldsymbol{d}^*)\tilde{a}(t) - \boldsymbol{\kappa}^\dagger C^{*-1}\tilde{\boldsymbol{s}}_+(t), \tag{15a}$$

$$\tilde{\boldsymbol{s}}_-(t) = C^{*-1}\tilde{\boldsymbol{s}}_+(t) - C^{*-1}\boldsymbol{d}^*\tilde{a}(t). \tag{15b}$$

Comparing Eqs. (15) and (10), we obtain the relationship between the TCMT descriptions of the original and conjugate systems.

$$\widetilde{C} = C^{*-1} \tag{16}$$

$$\widetilde{\boldsymbol{d}} = -C^{*-1}\boldsymbol{d}^* \tag{17}$$

$$\widetilde{\boldsymbol{\kappa}} = -C^{\dagger-1}\boldsymbol{\kappa}^* \tag{18}$$

$$\widetilde{\omega}_0 = \omega_0 + \mathrm{Im}(\boldsymbol{\kappa}^\dagger C^{*-1}\boldsymbol{d}^*) \tag{19}$$

$$\widetilde{\gamma} = -\gamma - \mathrm{Re}(\boldsymbol{\kappa}^\dagger C^{*-1}\boldsymbol{d}^*) \tag{20}$$

Equations (16 - 20) represent one of the main results of the paper. We note the consistency of Eqs. (16 - 20) obtained from the TCMT description above and the scattering matrix descriptions of the original and conjugate systems. The scattering matrix of a system describes the relationship between the amplitudes of the outgoing and incoming waves. For the original system, we have

$$\boldsymbol{s}_- = S\boldsymbol{s}_+. \tag{21}$$

From Eq. (21), we get

$$\boldsymbol{s}_+^* = S^{*-1}\boldsymbol{s}_-^*. \tag{22}$$

On the other hand, from Eqs. (12) and (13), we see that $\boldsymbol{s}_+^*$ and $\boldsymbol{s}_-^*$ correspond to outgoing and incoming waves in the conjugate system. Thus, the scattering matrix of the conjugate system $\widetilde{S}$ is

$$\widetilde{S} = S^{*-1}. \tag{23}$$

The scattering matrix of the original system can be obtained from the TCMT (Eq. (9)):

$$S = C + \frac{\boldsymbol{d}\boldsymbol{\kappa}^T}{i(\omega - \omega_0) + \gamma}. \tag{24}$$

Similarly, the scattering matrix of the conjugate system is obtained from Eq. (10):

$$\widetilde{S} = \widetilde{C} + \frac{\widetilde{\boldsymbol{d}}\widetilde{\boldsymbol{\kappa}}^T}{i(\omega - \widetilde{\omega}_0) + \widetilde{\gamma}}. \tag{25}$$

With the relations (Eqs. (16 - 20)), it is easy to show that:

$$\left[\widetilde{C} + \frac{\widetilde{\boldsymbol{d}}\widetilde{\boldsymbol{\kappa}}^T}{i(\omega - \widetilde{\omega}_0) + \widetilde{\gamma}}\right]\left[C^* + \frac{\boldsymbol{d}^*\boldsymbol{\kappa}^\dagger}{-i(\omega - \omega_0) + \gamma}\right] = I, \tag{26}$$

where I is the identity matrix. Thus, Eqs. (16 - 20) are consistent with Eq. (23).

In the above derivation, the frequency ω is assumed to be real. However, Eq. (23) can be easily extended to the complex frequencies. If we assume the incoming waves are at a complex frequency ω in the original scattering process in the original system, the frequency of the incoming waves in the time-reversed scattering process in the conjugate system is ω^*. Thus, Eq. (23) becomes

$$\widetilde{S}(\omega^*) = [S(\omega)]^{*-1}, \tag{27}$$

From Eq. (27), we find that the poles (zeros) of $\widetilde{S}$ in the complex frequency plane are complex conjugate of the zeros (poles) of S. This is consistent with the previous study of the scattering matrices in [24].

In Sections III - V, we will apply the general TCMT relations between the original and conjugate systems to establish some of the general constraints in TCMT for systems that satisfy time-reversal symmetry, energy conservation, or Lorentz reciprocity.

III. CONSTRAINTS ON THE TCMT IN SYSTEMS WITH TIME-REVERSAL SYMMETRY

In a system with time-reversal symmetry, its permittivity distribution satisfies $\boldsymbol{\epsilon}(\boldsymbol{r}) = \boldsymbol{\epsilon}^*(\boldsymbol{r})$, and hence its conjugate is the same system. Equations (16 - 20) become:

$$C = C^{*-1}, \tag{28}$$

$$\boldsymbol{d} = -C^{*-1}\boldsymbol{d}^*, \tag{29}$$

$$\boldsymbol{\kappa} = -C^{\dagger-1}\boldsymbol{\kappa}^*, \tag{30}$$

$$\omega_0 = \omega_0 + \mathrm{Im}(\boldsymbol{\kappa}^\dagger C^{*-1}\boldsymbol{d}^*), \tag{31}$$

$$\gamma = -\gamma - \mathrm{Re}(\boldsymbol{\kappa}^\dagger C^{*-1}\boldsymbol{d}^*). \tag{32}$$

Thus, we can get the following constraints on the TCMT description for systems with time-reversal symmetry.

$$CC^* = I \tag{33}$$

$$C\boldsymbol{d}^* + \boldsymbol{d} = 0 \tag{34}$$

$$C^T\boldsymbol{\kappa}^* + \boldsymbol{\kappa} = 0 \tag{35}$$

$$\boldsymbol{\kappa}^\dagger\boldsymbol{d} = 2\gamma \tag{36}$$

Equations (33 - 36) can also be derived from the properties of the scattering matrix, which can be found in Appendix A.

IV. CONSTRAINTS ON THE TCMT IN SYSTEMS WITH ENERGY CONSERVATION

In an energy conserving system, the permittivity of the material is a Hermitian tensor, i.e. $\boldsymbol{\epsilon} = \boldsymbol{\epsilon}^\dagger$. Its scattering matrix S is a unitary matrix:

$$S^\dagger S = I. \tag{37}$$

The permittivity of the time-reversed conjugate system is $\boldsymbol{\epsilon}^* = \boldsymbol{\epsilon}^T$. The conjugate system also satisfies energy conservation. Hence, the scattering matrix of the time-reversal conjugate system is [25]

$$\widetilde{S} = S^{*-1} = S^T. \tag{38}$$

Based on Eqs. (24), (25) and (38), we get

$$\widetilde{C} + \frac{\widetilde{\boldsymbol{d}}\widetilde{\boldsymbol{\kappa}}^T}{i(\omega - \widetilde{\omega}_0) + \widetilde{\gamma}} = C^T + \frac{\boldsymbol{\kappa}\boldsymbol{d}^T}{i(\omega - \omega_0) + \gamma}. \tag{39}$$

Since Eq. (39) holds for all frequencies near the resonance, the following relations must hold:

$$\widetilde{C} = C^T, \tag{40}$$

$$\widetilde{\boldsymbol{d}}\widetilde{\boldsymbol{\kappa}}^T = \boldsymbol{\kappa}\boldsymbol{d}^T, \tag{41}$$

$$\widetilde{\omega}_0 = \omega_0, \tag{42}$$

$$\widetilde{\gamma} = \gamma. \tag{43}$$

Substitute Eqs. (40), (42) and (43) into Eqs. (16), (19) and (20), one can obtain

$$C^\dagger C = I, \tag{44}$$

$$\boldsymbol{\kappa}^\dagger C^{*-1}\boldsymbol{d}^* = -2\gamma. \tag{45}$$

Combining Eqs. (18), (17) and (45), we have

$$\widetilde{\boldsymbol{\kappa}}^T\boldsymbol{d}^* = 2\gamma, \tag{46}$$

$$\boldsymbol{\kappa}^\dagger\widetilde{\boldsymbol{d}} = 2\gamma. \tag{47}$$

Moreover, energy conservation leads to [4]

$$\boldsymbol{d}^\dagger\boldsymbol{d} = 2\gamma. \tag{48}$$

Thus, we can multiply both sides of Eq. (41) by $\boldsymbol{d}^*$ and apply Eqs. (46) and (48) to get

$$\widetilde{\boldsymbol{d}} = \boldsymbol{\kappa}, \tag{49}$$

$$\widetilde{\boldsymbol{\kappa}} = \boldsymbol{d}. \tag{50}$$

From Eqs. (47) and (49), we have

$$\boldsymbol{\kappa}^\dagger\boldsymbol{\kappa} = 2\gamma. \tag{51}$$

We can substitute Eqs. (49) and (50) back to Eqs. (17) and (18) and use the unitary property of C to obtain

$$C^T\boldsymbol{d}^* + \boldsymbol{\kappa} = 0, \tag{52}$$

$$C\boldsymbol{\kappa}^* + \boldsymbol{d} = 0, \tag{53}$$

which are the same as the results derived in [21].

V. CONSTRAINTS ON THE TCMT IN SYSTEMS WITH LORENTZ RECIPROCITY

We now discuss the case of systems satisfying Lorentz reciprocity, where the dielectric tensors of the materials in the system are symmetric, i.e. $\boldsymbol{\epsilon}(\boldsymbol{r}) = \boldsymbol{\epsilon}^T(\boldsymbol{r})$. The total scattering matrix is symmetric ($S = S^T$) and consequently,

$$C + \frac{\boldsymbol{d}\boldsymbol{\kappa}^T}{i(\omega - \omega_0) + \gamma} = C^T + \frac{\boldsymbol{\kappa}\boldsymbol{d}^T}{i(\omega - \omega_0) + \gamma}. \tag{54}$$

The background scattering matrix C is also symmetric and $\boldsymbol{d}\boldsymbol{\kappa}^T = \boldsymbol{\kappa}\boldsymbol{d}^T$. Furthermore, we prove, in Appendix B, the following relation based on Lorentz reciprocity:

$$\boldsymbol{\kappa} = \boldsymbol{d}. \tag{55}$$

To summarize the results presented in Sections III - V, we have derived the constraints on the TCMT imposed separately by time-reversal symmetry, energy conservation and Lorentz reciprocity. The results are summarized in Table I.

System property	Scattering matrix	TCMT constraints
Time-reversal symmetry $\boldsymbol{\epsilon} = \boldsymbol{\epsilon}^*$	$SS^* = I$	$CC^* = I$ $\boldsymbol{\kappa}^\dagger\boldsymbol{d} = 2\gamma$ $C\boldsymbol{d}^* + \boldsymbol{d} = 0$ $C^T\boldsymbol{\kappa}^* + \boldsymbol{\kappa} = 0$
Energy conservation $\boldsymbol{\epsilon} = \boldsymbol{\epsilon}^\dagger$	$S^\dagger S = I$	$C^\dagger C = I$ $\boldsymbol{d}^\dagger\boldsymbol{d} = \boldsymbol{\kappa}^\dagger\boldsymbol{\kappa} = 2\gamma$ $C\boldsymbol{\kappa}^* + \boldsymbol{d} = 0$ $C^T\boldsymbol{d}^* + \boldsymbol{\kappa} = 0$
Lorentz reciprocity $\boldsymbol{\epsilon} = \boldsymbol{\epsilon}^T$	$S = S^T$	$C = C^T$ $\boldsymbol{\kappa} = \boldsymbol{d}$

TABLE I. Summary of the constraints on the TCMT imposed separately by time-reversal symmetry, energy conservation and Lorentz reciprocity.

VI. RELATION BETWEEN THE ORIGINAL AND TIME-REVERSAL CONJUGATE SYSTEM WITH LORENTZ RECIPROCITY

In this section we provide a numerical validation of our theory, by exploring some of the non-trivial consequence of Eqs. (16)-(20). For a closed system, where $\boldsymbol{\kappa} = \boldsymbol{d} = 0$, Eqs. (16)-(20) indicates that

$$\widetilde{\omega}_0 = \omega_0, \tag{56}$$

$$\widetilde{\gamma} = -\gamma. \tag{57}$$

In other word, the complex resonant frequencies of the original and the conjugate systems are complex conjugate of each other. In contrast, for an open system, Eqs. (56) and (57) no longer hold.

Specifically, we consider a reciprocal system with loss or gain in this section. The radiative decay rate is determined by the coupling coefficients:

$$\gamma_r = \boldsymbol{d}^\dagger\boldsymbol{d}/2. \tag{58}$$

The intrisic decay rate is thus

$$\gamma_i = \gamma - \gamma_r. \tag{59}$$

In our convention, positive decay rate represents loss, while negative decay rate represents gain. From Eqs. (17) and (20) as well as $\boldsymbol{\kappa} = \boldsymbol{d}$, which arises from reciprocity (Eq. (55)), we can find the relation between the intrinsic rates of the original and conjugate systems:

$$\begin{aligned}\widetilde{\gamma}_i + \gamma_i &= -\widetilde{\gamma}_r - \gamma_r + Re(\boldsymbol{d}^\dagger \tilde{\boldsymbol{d}}) \\ &= -\frac{1}{2}[\tilde{\boldsymbol{d}}^\dagger \tilde{\boldsymbol{d}} + \boldsymbol{d}^\dagger \boldsymbol{d} - \boldsymbol{d}^\dagger \tilde{\boldsymbol{d}} - \tilde{\boldsymbol{d}}^\dagger \boldsymbol{d}] \\ &= -\frac{1}{2}(\tilde{\boldsymbol{d}} - \boldsymbol{d})^\dagger (\tilde{\boldsymbol{d}} - \boldsymbol{d}) \leqslant 0.\end{aligned} \tag{60}$$

The equality holds for closed system where $\boldsymbol{d} = \tilde{\boldsymbol{d}} = 0$.

Suppose the original system has material loss. Its conjugate system hence has material gain. Equation (60) suggests that the intrinsic gain rate of the resonance in the time-reversal conjugate system should be larger than the intrinsic loss rate of the resonance in the original system. On the other hand, the non-resonant channels in the original system with material loss cannot amplify the input power. As a result, the eigenvalues of C lies either within or on the unit circle of the complex plane. In this situation, the radiative rate of the resonance in the conjugate system should be no less than the radiative rate of the resonance in the original system, which can be proven as following:

$$\begin{aligned}\widetilde{\gamma}_r - \gamma_r &= \frac{1}{2}[\tilde{\boldsymbol{d}}^\dagger \tilde{\boldsymbol{d}} - \boldsymbol{d}^\dagger \boldsymbol{d}] \\ &= \frac{1}{2}\boldsymbol{d}^\dagger [(CC^\dagger)^{-1} - I]\boldsymbol{d} \geqslant 0.\end{aligned} \tag{61}$$

Equations (60) and (61) are non-trivial consequences of our temporal coupled mode theory and arises due to the openness of the system. These relations are not intuitively obvious. We now proceed to provide a numerical check of these predictions, as a validation of the TCMT formalism discussed in the paper. As a concrete physical example, we study the guided resonance [3, 13] in a one-dimensional grating as shown in Fig. 2(a), which consists of a dielectric grating and a bottom slab. The relative permittivity of the grating is 12. The relative permittivity of the bottom slab is $2 - i\epsilon_i$. In the simulation, we vary ϵ_i, as well as the spacing between the grating and the bottom slab (g) and the width of the top grating ridge (w) to study the resonances in this system. An exemplary transmission spectrum for TM-polarization is shown in Fig. 2(c), with $\epsilon_i = 0.5$, $g = 0$, and $w = 0.2l$, where l is the periodicity of the grating. The spectrum exhibits multiple resonances. The electric field distribution of one of these resonances near the frequency of $0.52c/l$ is shown in Fig. 2(b). The field shows strong concentration in the dielectric grating region, as an indication of its guided resonance nature. Around each resonant mode, we numerically calculate the transmission and reflection spectrum using rigorous coupled wave analysis [26] and fit them with the TCMT to extract the TCMT parameters, i.e. C, $\boldsymbol{d}$, ω_0 and γ. To simulate the time-reversed conjugate system, we simply change the relative permittivity of the bottom slab to $2 + i\epsilon_i$ and repeat the same procedure as discussed above.

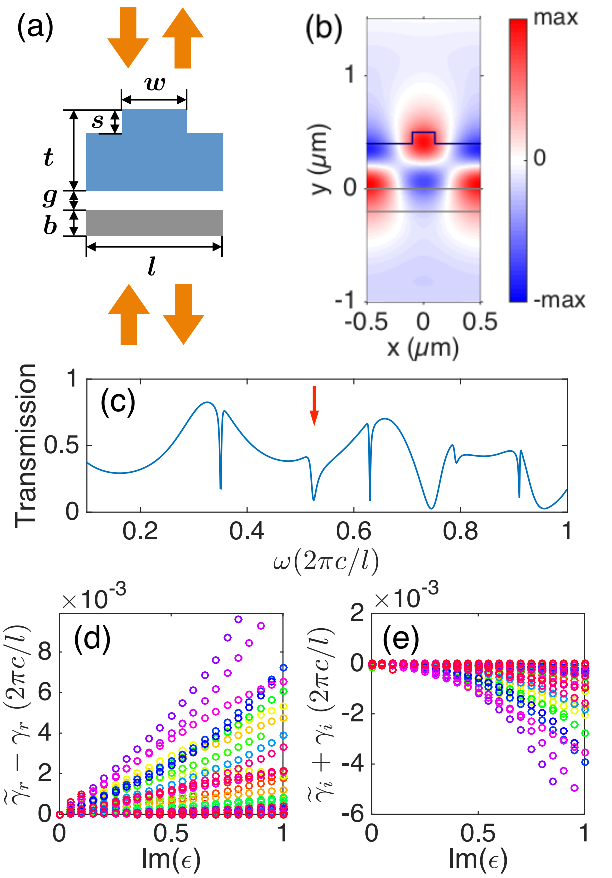

FIG. 2. (a) Schematic of a unit cell of a dielectric grating that supports guided resonances. The relative permittivity of the grating (in blue) is 12. The relative permittivity of the bottom slab (in grey) is $2 - i\epsilon_i$, where the imaginary part is varied. The periodicity is l, the grating total thickness $t = 0.5l$, the thickness of top grating ridge $s = 0.1l$, and the bottom slab thickness $b = 0.2l$. To sample different resonant modes, the gap between the grating and the bottom slab g is varied within 0 - $0.2l$, and the width of the top grating ridge w is varied within 0.2 - $0.8l$. Only TM modes at Γ points are studied. For example, with parameters $\epsilon_i = 0.5$, $g = 0$, and $w = 0.2l$, the electric field of a resonance near $\omega = 0.52 \times 2\pi c/l$ is shown in (b), and the transmission spectrum is shown in (c). (d) and (e) show $\widetilde{\gamma}_r - \gamma_r$ and $\widetilde{\gamma}_i + \gamma_i$ as a function of ϵ_i for different resonant modes, respectively.

The numerically obtained $\widetilde{\gamma}_r - \gamma_r$ and $\widetilde{\gamma}_i + \gamma_i$ are plotted in Fig. 2 (d) and (e) respectively. Each point represents one particular resonant mode. Fig. 2(d) clearly shows that all the points are above zero, which provides validation for Eq. (61) numerically. In Fig. 2(e), most of the points lie below zero, with some exceptions for small ϵ_i. This results from the numerical error, since γ_i

is obtained through subtracting two relatively large numbers (Eq. (59)). In spite of some small numerical errors, the numerical results provide evidence for the validity of Eq. (60).

VII. CONCLUSION

In conclusion, we establish a connection in the temporal coupled mode theory formalism for a resonant optical system and its time-reversal counter part. We make use of this connection to establish the constraint of time-reversal symmetry, energy conservation, and Lorentz reciprocity *separately* on the parameters of the temporal coupled mode theory. This connection also indicates some of the non-trivial implications on the relation between the resonant properties of a physical system and its time-reversal conjugate. Our work should deepen the understanding of the temporal coupled mode theory formalism, and also broaden the potential scope of application of such theory to a wider range of resonant systems.

ACKNOWLEDGEMENT

This work is supported by the Department of Energy under Grant No. DE-FG02-07ER46426. Z. Z acknowledges support from Stanford Graduate Fellowship and helpful discussions with Mr. Xiao-Qi Sun.

Appendix A: Derivation of the constraints on TCMT from the scattering matrix

In Sections III and IV, we derive the constraints on TCMT using the time-reversal conjugate system as an auxiliary. In this appendix, we start from the properties of the scattering matrix to derive the constraints on TCMT. A similar procedure is adopted in [21], and we re-derive some of the results in [21] for completeness.

In a system satisfying time-reversal symmetry, the scattering matrix satisfies $SS^* = I$, where the form of the scattering matrix as determined by the TCMT description is given in Eq. (24). Thus, the following relations hold over the frequency range around the resonance.

$$\left[C + \frac{\boldsymbol{d}\boldsymbol{\kappa}^T}{i(\omega-\omega_0)+\gamma}\right]\left[C^* + \frac{\boldsymbol{d}^*\boldsymbol{\kappa}^\dagger}{-i(\omega-\omega_0)+\gamma}\right] = I. \quad \text{(A1)}$$

Since the background channel also satisfies the time-reversal symmetry, we have $CC^* = I$. Thus, Eq. (A1) leads to

$$(C\boldsymbol{d}^*)\boldsymbol{\kappa}^\dagger - \boldsymbol{d}(C^T\boldsymbol{\kappa}^*)^\dagger = 0, \quad \text{(A2)}$$

$$\gamma[(C\boldsymbol{d}^*)\boldsymbol{\kappa}^\dagger + \boldsymbol{d}(C^T\boldsymbol{\kappa}^*)^\dagger] + \boldsymbol{\kappa}^T\boldsymbol{d}^*\boldsymbol{d}\boldsymbol{\kappa}^\dagger = 0. \quad \text{(A3)}$$

Consider a process where the resonant mode has non-zero amplitude at $t = 0$, and decays with no incident waves [4]. From Eq. (9), the outgoing waves are

$$\boldsymbol{s}_- = \boldsymbol{d}a. \quad \text{(A4)}$$

In the time-reversed process, the amplitude of the resonance is a^*, and the incoming and outgoing waves are $\boldsymbol{s}_+ = \boldsymbol{d}^*a^*$ and $\boldsymbol{s}_- = 0$ respectively. The time-reversed process is described by the TCMT with the same parameters, since the system has time-reversal symmetry. Thus, $0 = C\boldsymbol{d}^*a^* + \boldsymbol{d}a^*$, and we get

$$C\boldsymbol{d}^* + \boldsymbol{d} = 0. \quad \text{(A5)}$$

Substitute Eq. (A5) into Eqs. (A2) and (A3), we obtain

$$C^T\boldsymbol{\kappa}^* + \boldsymbol{\kappa} = 0, \quad \text{(A6)}$$

$$\boldsymbol{\kappa}^\dagger\boldsymbol{d} = 2\gamma. \quad \text{(A7)}$$

Therefore, we reproduce the first row in Table I.

We proceed to apply the same procedure to study systems satisfying energy conservation. The scattering matrix is unitary, i.e. $S^\dagger S = I$, and so is the background scattering matrix $C^\dagger C = I$. With the form of the scattering matrix presented in Eq. (24), we have:

$$\left[C^\dagger + \frac{\boldsymbol{\kappa}^*\boldsymbol{d}^\dagger}{-i(\omega-\omega_0)+\gamma}\right]\left[C + \frac{\boldsymbol{d}\boldsymbol{\kappa}^T}{i(\omega-\omega_0)+\gamma}\right] = I, \quad \text{(A8)}$$

which holds over the frequency range around the resonance. Thus,

$$\boldsymbol{\kappa}^*(C^\dagger\boldsymbol{d})^\dagger - (C^\dagger\boldsymbol{d})\boldsymbol{\kappa}^T = 0, \quad \text{(A9)}$$

$$\gamma[\boldsymbol{\kappa}^*(C^\dagger\boldsymbol{d})^\dagger + (C^\dagger\boldsymbol{d})\boldsymbol{\kappa}^T] + \boldsymbol{d}^\dagger\boldsymbol{d}\boldsymbol{\kappa}^*\boldsymbol{\kappa}^T = 0. \quad \text{(A10)}$$

From Eq. (A9), we can get

$$C^\dagger\boldsymbol{d} = \alpha\boldsymbol{\kappa}^*, \quad \text{(A11)}$$

where α is a real number.

Similar to the derivation for the time-reversal symmetry case, here, we consider again the process that the resonance has a non-zero amplitude at $t = 0$, and decays at $t > 0$ with no incident waves [4]:

$$\frac{d}{dt}a = (i\omega_0 - \gamma)a, \quad \text{(A12)}$$

$$\boldsymbol{s}_- = \boldsymbol{d}a. \quad \text{(A13)}$$

Since energy is conserved, the decay per unit time for the energy in the resonance should be equal to the power carried by the outgoing waves, i.e. $\frac{d}{dt}|a|^2 = -\boldsymbol{s}_-^\dagger\boldsymbol{s}_-$. So, we get

$$\boldsymbol{d}^\dagger\boldsymbol{d} = 2\gamma. \quad \text{(A14)}$$

Substitute Eqs. (A11) and (A14) into Eq. (A10), we find that $\alpha = -1$ and

$$C^\dagger\boldsymbol{d} + \boldsymbol{\kappa}^* = 0. \quad \text{(A15)}$$

Based on the unitarity of C, Eqs. (A14) and (A15) lead to

$$\boldsymbol{\kappa}^\dagger\boldsymbol{\kappa} = 2\gamma, \quad \text{(A16)}$$

$$C\boldsymbol{\kappa}^* + \boldsymbol{d} = 0. \quad \text{(A17)}$$

We have therefore re-derived the second row of Table I based on the scattering matrix.

Appendix B: Derivation of $\boldsymbol{\kappa} = \boldsymbol{d}$ in a Lorentz reciprocal system

In this Appendix, we derive $\boldsymbol{\kappa} = \boldsymbol{d}$ in a Lorentz reciprocal system. We construct two field solutions to Maxwell's equations. In the first case, the electromagnetic fields ($\boldsymbol{E}$ and $\boldsymbol{H}$) are excited by a current density distribution $\boldsymbol{J}$, which excites a waveguide mode in port l. In the second case, the electromagnetic fields ($\bar{\boldsymbol{E}}$ and $\bar{\boldsymbol{H}}$) are excited by a current density distribution $\bar{\boldsymbol{J}}$, which is a dipole source located within the resonator.

We can assume that each port coupling to the resonator is tapered to be a weakly guided waveguide far away from the resonator. Thus, the guided mode resembles a plane wave locally and satisfies the approximation $\boldsymbol{h}_i \approx \boldsymbol{n}_i \times \boldsymbol{e}_i/\eta_i$, where η_i is the impedance of the weakly guided waveguide connecting port i, $\boldsymbol{n}_i$ is the unit vector normal to the waveguide cross section, and $\boldsymbol{e}_i$, $\boldsymbol{h}_i$ are the normalized waveguide mode, such that

$$\frac{1}{2}\mathrm{Re}\int_{A_i} \boldsymbol{e}_i \times \boldsymbol{h}_i^* \cdot dS = 1. \tag{B1}$$

With the approximation that $\boldsymbol{h}_i \approx \boldsymbol{n}_i \times \boldsymbol{e}_i/\eta_i$ and proper choice of the phase such that $\boldsymbol{e}_i$ is real, the normalization equation becomes

$$\frac{1}{2\eta_i}\int_{A_i} \boldsymbol{e}_i^T \boldsymbol{e}_i dS = 1. \tag{B2}$$

In the first case, the current density amplitude is $\boldsymbol{J} = -2\boldsymbol{e}_l/\eta_l \times \delta(z - z_1)$, lying on one cross section at z_1 of the waveguide connecting to port l, with frequency ω, where z parameterizes the distance along the waveguide. The incident power from port l has amplitude unity, i.e. $s_{+i} = \delta_{il}$. Thus, the amplitude of the resonant mode in the first case is

$$a_1 = \frac{\kappa_l}{i(\omega - \omega_0) + \gamma}. \tag{B3}$$

We can further set the current oscillation frequency equal to the resonant frequency of the single-mode resonator. Then, $a_1 = \kappa_l/\gamma$. Suppose the electric field distribution of the resonant mode is $\boldsymbol{E}_0(r)$. The field $\boldsymbol{E}$ excited by the current $\boldsymbol{J}$ is approximately

$$\boldsymbol{E}(r) = \xi a_1 \boldsymbol{E}_0(r), \tag{B4}$$

where $\xi = \left(\frac{1}{2}\int \boldsymbol{E}_0^\dagger(r)\mathrm{Re}[\epsilon(r)]\boldsymbol{E}_0(r)dr\right)^{-1/2}$ is a coefficient for energy normalization.

In the second case, the field is excited by a dipole located at $\boldsymbol{r}_2$ oscillating at the resonant frequency ω_0, as described by a current density $\bar{\boldsymbol{J}} = \boldsymbol{J}_2\delta(\boldsymbol{r} - \boldsymbol{r}_2)$. Suppose that the dipole mainly excites the resonant mode. The field $\bar{\boldsymbol{E}}(r)$ is proportional to $\boldsymbol{E}_0(r)$, i.e. $\bar{\boldsymbol{E}}(r) = \zeta\boldsymbol{E}_0(r)$ [27, 28], where ζ is a coefficient. The amplitude of the resonant mode in this case is $a_2 = \zeta/\xi$. The total energy decay rate is equal to the power radiated from the dipole source. Thus,

$$-\frac{1}{2}\mathrm{Re}[\zeta^* \boldsymbol{E}_0^\dagger(r_2)\boldsymbol{J}_2] = 2\gamma|\zeta|^2\xi^{-2}, \tag{B5}$$

where γ is the total decay rate and ξ is the energy normalization coefficient. We can choose the global phase for the field distribution of the resonant mode such that $\boldsymbol{E}_0(r_2)$ is real and positive along the direction of the dipole current $\boldsymbol{J}_2$. Then we can find $\zeta = -(\xi^2/4\gamma)\boldsymbol{E}_0^T(r_2)\boldsymbol{J}_2$ from Eq. (B5). The field in this case is

$$\bar{\boldsymbol{E}}(r) = -\frac{1}{4\gamma}\xi^2\boldsymbol{E}_0^T(r_2)\boldsymbol{J}_2\boldsymbol{E}_0(r). \tag{B6}$$

Comparing Eqs. (B4) and (B6), we can find that the amplitude of the resonant mode in the second case is

$$a_2 = -\frac{1}{4\gamma}\xi\boldsymbol{E}_0^T(r_2)\boldsymbol{J}_2. \tag{B7}$$

Consequently, the amplitudes of the outgoing waves are

$$s_{-i} = d_i a_2 = -\frac{1}{4\gamma}\xi\boldsymbol{E}_0^T(r_2)\boldsymbol{J}_2 d_i. \tag{B8}$$

And the field in the waveguide connecting port l is $s_{-i}\boldsymbol{e}_l$.

In a system satisfying Lorentz reciprocity, the two sets of field solutions ($\boldsymbol{E}$, $\boldsymbol{H}$) and ($\bar{\boldsymbol{E}}$, $\bar{\boldsymbol{H}}$), respectively excited by current $\boldsymbol{J}$ and $\bar{\boldsymbol{J}}$, satisfy the following relation [29].

$$\int_{\partial V}(\boldsymbol{E}\times\bar{\boldsymbol{H}} - \bar{\boldsymbol{E}}\times\boldsymbol{H})\cdot d\boldsymbol{S} = \int dV(\bar{\boldsymbol{E}}\cdot\boldsymbol{J} - \boldsymbol{E}\cdot\bar{\boldsymbol{J}}) \tag{B9}$$

By putting reciprocal absorption materials far away from the resonator and waveguides, the left hand side of Eq. (B9) vanishes. Substitute the fields and currents in the first and the second cases into Eq. (B9),

$$\int_{A_l}\left[-\frac{\xi}{4\gamma}\boldsymbol{E}_0^T(r_2)\boldsymbol{J}_2 d_l\boldsymbol{e}_l^T\right]\left[-\frac{2}{\eta_l}\boldsymbol{e}_l\right] = \xi\frac{\kappa_l}{\gamma}\boldsymbol{E}_0^T(r_2)\boldsymbol{J}_2. \tag{B10}$$

With the normalization condition (Eq. (B2)), we find that

$$d_l = \kappa_l, \tag{B11}$$

where l can be any one of the ports. Consequently, we show that $\boldsymbol{d} = \boldsymbol{\kappa}$.

[1] H. A. Haus and W. Huang, Proceedings of the IEEE **79**, 1505 (1991).

[2] H. A. Haus, *Waves and fields in optoelectronics*

(Prentice-Hall, 1984).
[3] J. D. Joannopoulos, S. G. Johnson, J. N. Winn, and R. D. Meade, *Photonic crystals: molding the flow of light* (Princeton University Press, 2011).
[4] S. Fan, W. Suh, and J. D. Joannopoulos, J. Opt. Soc. Am. A **20**, 569 (2003).
[5] W. Suh, Z. Wang, and S. Fan, IEEE Journal of Quantum Electronics **40**, 1511 (2004).
[6] Z. Ruan and S. Fan, Physical Review A **85**, 043828 (2012).
[7] Z. Ruan and S. Fan, The Journal of Physical Chemistry C **114**, 7324 (2009).
[8] A. Karalis and J. Joannopoulos, Applied Physics Letters **107**, 141108 (2015).
[9] Z. Yu, A. Raman, and S. Fan, Proceedings of the National Academy of Sciences **107**, 17491 (2010).
[10] L. Verslegers, Z. Yu, Z. Ruan, P. B. Catrysse, and S. Fan, Physical Review Letters **108**, 083902 (2012).
[11] S. Assawaworrarit, X. Yu, and S. Fan, Nature **546**, 387 (2017).
[12] M. Zhou, S. Yi, T. S. Luk, Q. Gan, S. Fan, and Z. Yu, Physical Review B **92**, 024302 (2015).
[13] S. Fan and J. D. Joannopoulos, Phys. Rev. B **65**, 235112 (2002).
[14] Z. Ruan and S. Fan, Physical Review Letters **105**, 013901 (2010).
[15] C. Guo, M. Xiao, M. Minkov, Y. Shi, and S. Fan, Optica **5**, 251 (2018).
[16] H. Zhou, B. Zhen, C. W. Hsu, O. D. Miller, S. G. Johnson, J. D. Joannopoulos, and M. Soljačić, Optica **3**, 1079 (2016).
[17] H. Y. Song, S. Kim, and R. Magnusson, Optics express **17**, 23544 (2009).
[18] D. L. Sounas and A. Alú, Physical Review Letters **118**, 154302 (2017).
[19] S. Longhi, Physical Review A **82**, 031801 (2010).
[20] L. Feng, R. El-Ganainy, and L. Ge, Nature Photonics **11**, 752 (2017).
[21] K. X. Wang, Optics Letters **43**, 5623 (2018).
[22] Y. D. Chong, L. Ge, H. Cao, and A. D. Stone, Physical Review Letters **105**, 053901 (2010).
[23] D. G. Baranov, A. Krasnok, T. Shegai, A. Alù, and Y. D. Chong, Nature Reviews Materials **2**, 17064 (2017).
[24] Y. D. Chong, L. Ge, and A. D. Stone, Physical Review Letters **106**, 093902 (2011).
[25] M. Tamagnone, A. Fallahi, J. R. Mosig, and J. Perruisseau-Carrier, Nature photonics **8**, 556 (2014).
[26] V. Liu and S. Fan, Computer Physics Communications **183**, 2233 (2012).
[27] C. Sauvan, J.-P. Hugonin, I. S. Maksymov, and P. Lalanne, Physical Review Letters **110**, 237401 (2013).
[28] Z. Zhao, Y. Shi, K. Chen, and S. Fan, Physical Review A **98**, 013845 (2018).
[29] A. W. Snyder and J. Love, *Optical waveguide theory* (Springer Science & Business Media, 2012).